

Applicability of Radiowave Anechoic Chambers for Acoustic Free-Field Measurements on the Example of the Chamber at ITMO University

Farid Bismukhametov^{a,b}, Ksenia Razrezova^c, Roman Smolnitsky^c, Yuri Shchelokov^c, Nikolay Kanev^d and Mariia Krasikova^{e,a}

^aSchool of Physics and Engineering, ITMO University, Saint Petersburg, 197101, Russia

^bLaboratory "Acoustics of Halls", Research Institute of Building Physics, Moscow, 127238, Russia

^cSoundproofing European Technologies LLC, Saint Petersburg, 195027, Russia

^dDepartment of Architectural and Structural Design and Environmental Physics, Moscow State University of Civil Engineering, Moscow, 129337, Russia

^eDevolm LLC, Krasnoyarsk, 660049, Russia

ARTICLE INFO

Keywords:

acoustic anechoic chamber
radiowave anechoic chamber
free-field measurements

Abstract

Acoustic anechoic chambers allow free-field measurements required for the verification of effects under investigation and for the characterization of developing devices. However, the construction of an anechoic chamber is a labor-intensive process that requires a lot of resources, which is why these facilities are rather rare. An analogous statement can be made about radiowave chambers. At the same time, it is known that materials for radiowave absorption might absorb acoustic waves as well, and it can be expected that some chambers can be utilized for both electromagnetic and acoustic free-field measurements. This work examines the feasibility of the radiowave anechoic chamber of ITMO University (Saint-Petersburg, Russia) for acoustic measurements. The acoustic properties of the chamber coatings are estimated via measurements and numerical calculations. Characterization of sound pressure level, background noise level, and reverberation time is performed in accordance with the ISO 3745:2012 standard. The key conclusion is that the chamber can be considered as an acoustic anechoic chamber, but only for specific frequency ranges and distances from the source, which depend on the measurement directions.

1. Introduction

An essential stage of research and development work is the characterization of the systems under development, which typically requires high-precision measurements. Many of the testing procedures must be conducted under the free-field condition, when the amplitude is inversely proportional to the distance from the source [1]. When this condition is satisfied, it can be assumed that waves reflected from the surfaces of the surrounding space do not affect the results of measurements. For example, free-field conditions are required to determine the directivity and amplitude-frequency characteristics of loudspeakers [2], perform microphone calibration [3, 4], characterize musical instruments [5], test hearing aids [6] or investigate noise barriers [7, 8, 9, 10].

Free-field conditions can be implemented for measurements conducted in anechoic chambers representing rooms in which the scattering is suppressed by using absorbing coatings covering the surfaces of the

room [11]. Depending on the locations of the absorbing coatings, chambers can be classified into two types: semi-anechoic and fully anechoic. In the first case, the coatings cover the walls and ceiling of the chamber, while in the second case the floor is also covered to minimize the influence of reflections on the measurements. Usually, coatings are represented by arrays of wedges made of porous materials, such as glass wool [12], fiberglass [13, 14, 15, 16], ultra-fine basalt fiber [17], or phenolic felt [18]. At the same time, despite the abundance of various sound-absorbing materials, the quest to find the most efficient one is still open [19, 20, 21, 22, 23].

While anechoic chambers are crucially important facilities for acoustic measurement and testing, each camera represents a rather unique object [24, 13, 18, 25, 26], as the construction of the chambers is a laborious and resource intensive process. At the same time, anechoic chambers are constructed not only for acoustic measurements but also for electromagnetic ones [11]. The coatings absorbing radio-waves can be made of carbon-impregnated polyurethane [27], ferrite [28, 29], foil-coated polymers [30], or activated charcoal made of coconut shells [31]. It is noteworthy that some materials can absorb both acoustic and radio-waves. These might be carbon fibers [32], polymer nanocomposites [33],

 f.bismukhametov@metalab.ifmo.ru (F.

Bismukhametov); mariia.krasikova@gmail.com (M. Krasikova)
orcid(s): 0009-0004-6950-9216 (F. Bismukhametov);
0000-0001-6512-7131 (N. Kanev); 0000-0002-5950-4807 (M. Krasikova)

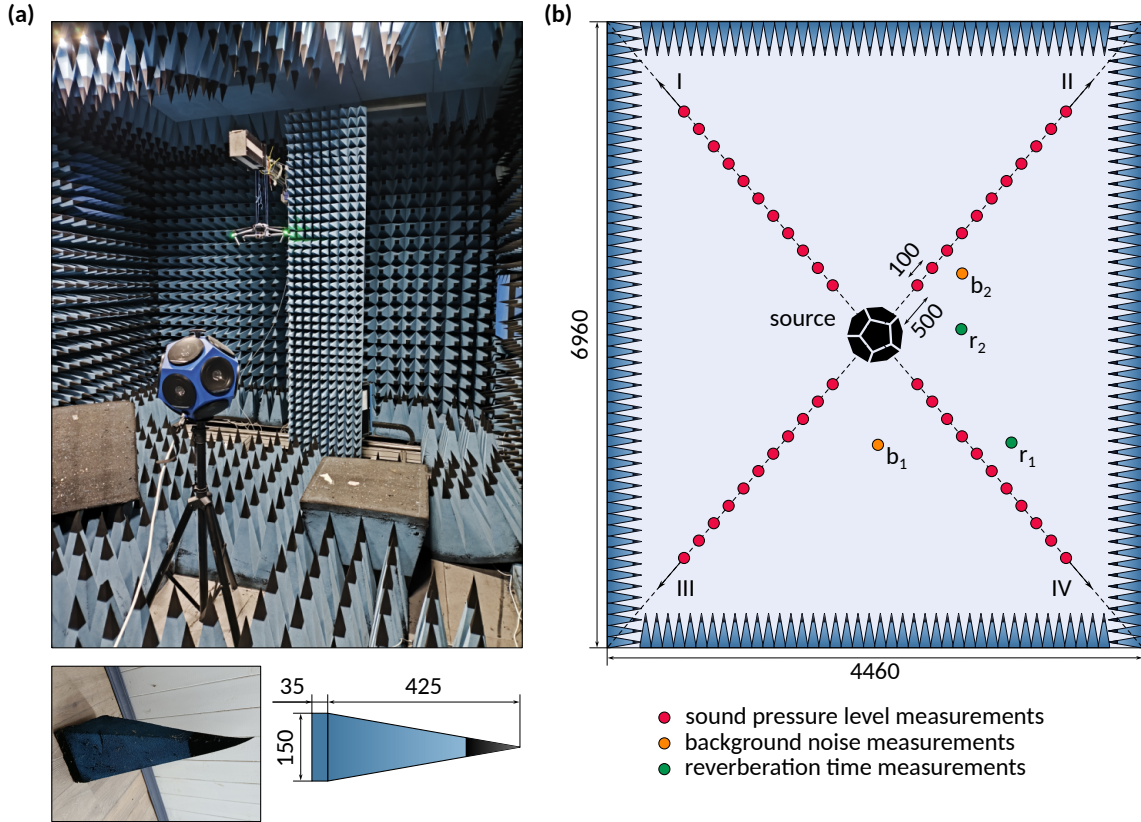


Figure 1: Considered system. (a) Photo of the anechoic chamber as well as photo and the schematic image of a pyramid element of the absorbing coating. (b) Measurement scheme with marked points at which the sound pressure level (red dots), background noise (orange dots) and reverberation time (green dots) are measured. The measurement directions are marked by indexes I – IV.

charcoal [34, 35], or metamaterials [36, 37]. Therefore, it can be expected that in some spectral ranges radio-wave anechoic chambers can be considered as acoustic ones and vice versa.

The aim of the work is to determine the suitability of the radio-wave anechoic chamber of ITMO University (Saint-Petersburg, Russia) for free-field acoustic measurements. Characterization of the chamber is performed in accordance with the ISO 3745:2012 / GOST-ISO 3745-2014 standard, which defines the requirements imposed on the sound pressure levels and background noise level. Additionally, acoustic absorption coefficient of the chamber coatings is estimated. It is demonstrated that the chamber can be utilized as an acoustic anechoic chamber in the case of measurements near the sound source (at the distances up to 0.9 m) at the frequencies up to 3150 Hz. The free-field condition is also satisfied for wider spectral ranges and at larger distances from the source, but whether the criteria for acoustic chambers are satisfied depends on the measurement directions. Therefore, the main conclusion of the work is that the radio-wave anechoic chamber of ITMO University is suitable for acoustic measurements under the free-field conditions at specific spectral ranges.

2. Description of the chamber

The chamber represents a room having the shape of a rectangular parallelepiped. Without coatings, the length of the walls is 4.46 and 6.96 m, and the height of the ceiling is 3.3 m. The coatings represent arrays of pyramid elements with a square base [see Fig. 1(a)], which are made of open cell foam rubber saturated with finely-dispersed carbon particles with admixture of metal oxides (about 2 – 3%). The height of each pyramid is 425 mm, while the thickness of the base is 35 mm, and the width of the base is 150 mm. To improve the radio-wave absorption, the apex parts are treated with a special solution the composition of which is unknown. It should be noted that there is a recess in the floor of the chamber that is 0.15 m deep, 1.3 m wide and 3.55 m long. Due to operational necessity, the recess is not covered by the absorbing coatings, as can be seen in Fig. 1(a). In addition, some parts of the ceiling are covered with uniform layers instead of pyramid arrays.

3. Methods

The determination of the acoustic characteristics of the chamber is provided in accordance with ISO 3745:2012 / GOST-ISO 3745-2014 [38, 39]. Pressure fields are generated by the omnidirectional sound

source OED-SP360 with the amplifier OED-PA360. Measurements of spatial distributions of the sound pressure level (SPL) are performed with the sound level meter Bruel&Kjaer type 2250 and the microphone Sennheiser e604. The background noise and reverberation time measurements are conducted in points $b_{1,2}$ and $r_{1,2}$, respectively, while the SPL measurements are carried out in several points located along 4 trajectories directed from the source to the corners of the camera, as shown in Fig. 1(b). Specifically, each measurement direction contains 11 points such that the closest to the source is located at the distance 500 mm from it, and the consequent points are arranged with the step 100 mm. The measurement time at each point is 30 s.

Measurements of the absorption coefficient of the coating material are conducted in the impedance tube using the two-microphone method, in accordance with ISO 10534-2:2023 [40]. The tube is characterized by a circular cross-section with radius 55 mm. The sound source is placed at one end of the tube, whereas the sample is at the other. Acoustic pressure is measured by microphones located at the distances 730 and 790 mm from the sample. Then, the transfer function is calculated to estimate the reflection coefficient R and the absorption coefficient $A = 1 - R$. The spectral range within which the reliable results can be obtained is limited by the geometry of the tube as high frequencies are associated with the excitation of non-piston modes. Specifically, the upper frequency is set to be 1800 Hz.

Numerical simulations are conducted with the help of COMSOL Multiphysics using the ‘‘Pressure Acoustics, Frequency Domain’’ module. The incident field is introduced as a plane wave with the amplitude 0.1 Pa using the ‘‘Background Pressure Field’’ feature. The absorption coefficient is calculated as $A = 1 - |r|^2$, where r is the reflection coefficient defined as

$$r = \frac{1}{V} \int \frac{p_s}{p_b} dV, \quad (1)$$

where p_s is the pressure of the scattered field, p_b is the pressure of the background (incident) field, and the integration is performed over a small closed volume V [see. Fig 2(c)].

4. Results

4.1. Absorbing Coatings

Due to limitations imposed by the dimensions of the measurement setup, the acoustic characteristics of the pyramid elements could not be estimated experimentally. Instead, the absorption coefficient of the coating material is measured for the disk-like sample cut from a pyramid. The radius of the sample is 55 mm, and the thickness is 25 mm. According to the results of measurements shown in Fig. 2(a), the absorption coefficient takes values from 0.17 to 0.5 within the spectral range 290 – 1800 Hz.

Table 1

Fitted values of flow resistivity of coating material for different empirical models.

Model	Flow resistivity (Pa·s/m ²)
Delany-Bazley	3437
Miki	5994
Mechel	5136
Garai-Pompoli	6125
JCA	8701

Since the sample is made of a porous material, its acoustic characteristics can be described using conventional empirical models in which the impedance and wavenumber are defined using flow resistivity σ . In particular, the experimental date is approximated by estimating the appropriate value of σ within the framework of the five most common models, such that the fitting accuracy is evaluated by calculating the standard deviation. The results of the estimations are listed in Tab 1. It can be stated that the Delany-Bazley model [41] provides the most accurate fitting, as shown in Fig. 2(a). An almost identical result is achieved using the Johnson-Champoux-Allard (JCA) [42] and Garai-Pompoli models [43]. Meanwhile, the Miki [44] and Mechel [45] models provide a bit worse result, but the deviation is small, as follows from Fig. 2(b).

Nevertheless, absorbing coatings are made of pyramid elements rather than uniform layers with a fixed thickness. At the same time, pyramid elements are known to have higher absorption compared to a non-structured layer of a porous material [46]. The estimation of the absorption coefficient is performed using numerical calculations. Specifically, a waveguide with a square cross section is considered such that the pyramid is placed at one end, while the second end is supplemented by the perfectly matched layer (PML). To imitate an infinitely periodic (along y and z axes) structure, Floquet periodicity conditions are imposed on the boundaries of the computational domain that lie in the xy and xz planes. The porous material is described with the Delany-Basley model with flow resistivity 3437 Pa · s/m² defined in the fitting step. Calculations are performed for both the disk and the pyramid samples. Note that the influence of the solution with which the apex is treated is not taken into account, and the pyramid is considered to be uniform.

According to Fig. 2(d), the results of calculations for the disk are expectedly close to the analytical approximation. The absorption coefficient in this case is below 0.5 for the whole considered spectral range. The situation changes drastically for the pyramid element, such that at 290 Hz the absorption coefficient is about 0.815 and then increases to 0.996 with increasing frequency. The spectral dependence in this case resembles

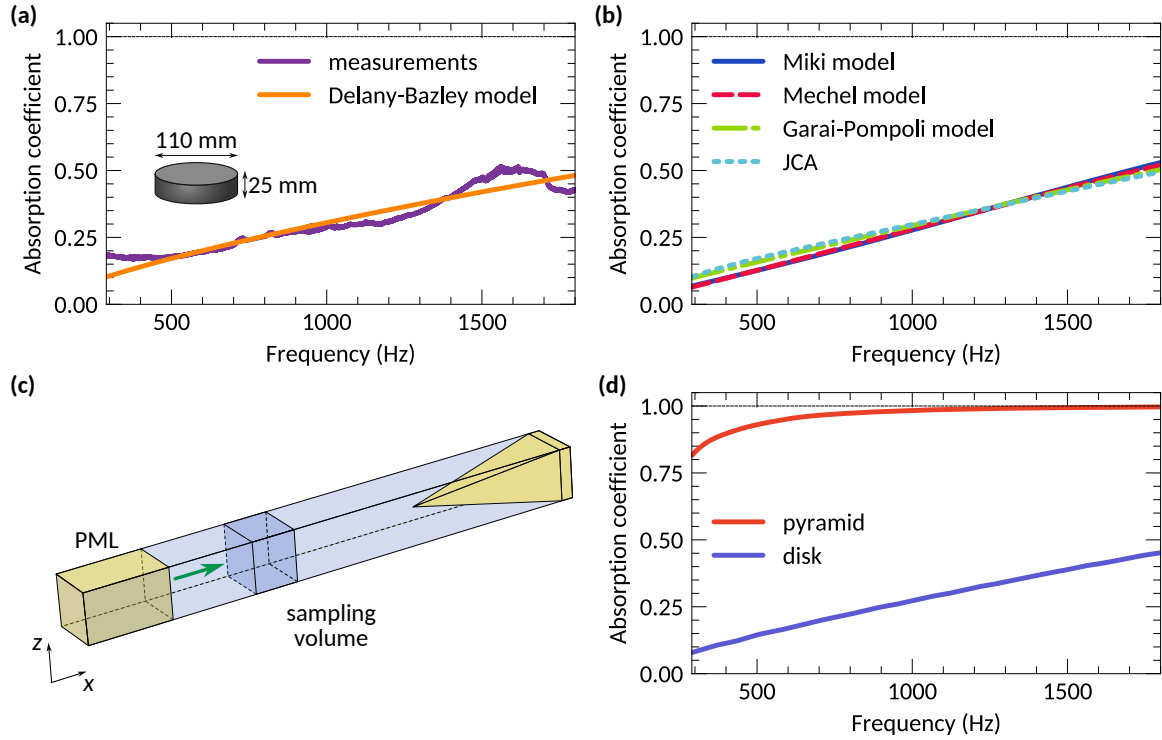


Figure 2: Acoustic properties of the coatings. (a) Measured absorption coefficient of the coating material and its approximation via Delany-Bazley model. The sample represents a disk with the radius 55 mm and the thickness 25 mm. (b) Approximation of the absorption coefficient using different empirical models. (c) Schematic illustration of the numerical model for calculation of absorption coefficient spectra of pyramid elements. Floquet periodicity conditions are imposed on the boundaries of the computational domain lying in xy and xz planes. (d) Numerically calculated absorption coefficient for the disk and pyramid samples characterized by the material with the flow resistivity $3437 \text{ Pa} \cdot \text{s}/\text{m}^2$ in the framework of the Delany-Bazley model.

a logarithmic function such that the absorption coefficient starts to overcome the value of 0.9 at frequencies above 410 Hz.

Therefore, it can be concluded that in terms of acoustic characteristics, chamber coatings are characterized by a reasonably high absorption coefficient (within the considered spectral range 290 – 1800 Hz) comparable to the one of materials utilized for coatings of acoustic anechoic chambers [47, 48, 49, 50, 51].

4.2. Background noise

One of the key characteristics of anechoic chambers is the background noise level, as it directly affects the results of conducted tests and measurements. According to ISO 3745:2012 / GOST-ISO 3745-2014, the requirements imposed on the background noise level are satisfied when the equivalent SPL of the background noise, averaged over the measurement points, is at least 10 dB lower than the corresponding equivalent SPL of the noise source for third-octave bands with center frequencies ranging from 250 to 5000 Hz.

The comparison of the measured equivalent SPL of the background noise and the noise source is shown in Fig. 3. On average, the SPL of the background noise is 72 dB than SPL of the source, such that the minimal difference is 65.7 dB (within the range 250 – 5000 Hz).

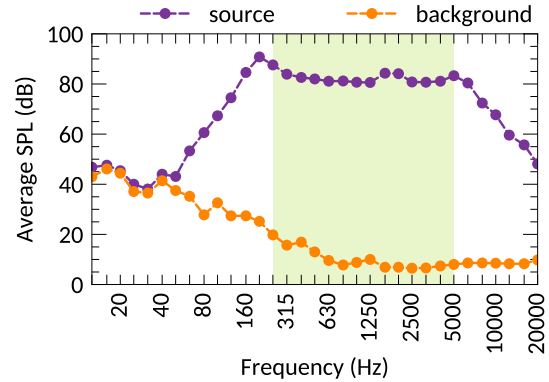


Figure 3: Background noise level. Spectra of the averaged equivalent sound pressure levels (SPL) of background noise and the equivalent SPL of the utilized noise source. Measurements are carried out at the center frequencies of the third-octave bands. Shaded area indicates the spectral range from 250 to 5000 Hz.

Hence, the requirements imposed on the background noise level are fully satisfied.

4.3. Reverberation time

Reverberation time defines the rate of SPL decrease after the switching off of the source. Therefore, the

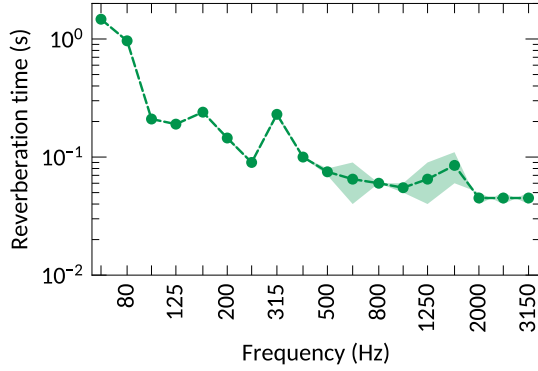


Figure 4: Measured reverberation time. The figure shows averaged reverberation time in the 1/3-octave frequency band. Shaded area indicates the spread of values.

lower the reverberation time, the smaller influence the reflected fields have on the total field distribution in the chamber. For an ideal anechoic chamber the reverberation time is equal to 0 s.

For the considered chamber, the reverberation time is the average of the reverberation times measured at two points marked in Fig. 1(b). The resulting spectrum (in the one-third octave bands) is shown in Fig. 4. According to the obtained dependence, the reverberation time quickly drops from 1.5 s at 63 Hz to 0.21 s at 100 Hz, and for the larger frequencies it remains in-between 0.05 and 0.24 s.

4.4. Sound Pressure Levels

The SPL spectra measured for various distances from the noise source are shown in Fig. 5. Crucially, the SPL for different measurement directions deviate from each other, which is an indication of the field inhomogeneities caused by reflections from the chamber walls. Therefore, it might be expected that the criteria for the chamber's suitability for different measurement directions will be met for different spectral ranges and distances from the source. In addition, it should be mentioned that the inequivalence of measurement directions can be related to non-uniformities in the directivity pattern of the source, which was not verified before the measurements. However, the conclusions of the work are based on the assumption that the source is omnidirectional.

The compliance of the chamber with the criteria imposed on anechoic chambers is defined by the comparison of measured SPL with the corresponding theoretical values calculated as

$$L_p(r_i) = 20 \lg \left(\frac{a}{r_i - r_0} \right), \quad (2)$$

where a is a parameter determined by the sound power of the noise source and r_0 is the displacement of the acoustic center along the trajectory of the microphone displacement from the origin (i.e. the center of the measurement spherical surface) from which the distance r_i

Table 2

The maximum acceptable deviations of measured sound pressure levels from the theoretical values.

Central frequency of the one-third octave band (Hz)	Acceptable deviations (dB)
≤ 630	± 1.5
from 800 to 5000	± 1.0
≥ 6300	± 1.5

is counted. These parameters can be defined as

$$a = \frac{M r_0^2 + \sum_{i=1}^M r_i^2 - 2 r_0 \sum_{i=1}^M r_i}{\sum_{i=1}^M r_i q_i - r_0 \sum_{i=1}^M q_i}, \quad (3)$$

$$r_0 = \frac{\sum_{i=1}^M r_i \sum_{i=1}^M r_i q_i - \sum_{i=1}^M r_i^2 \sum_{i=1}^M q_i}{\sum_{i=1}^M r_i \sum_{i=1}^M q_i - M \sum_{i=1}^M r_i q_i}, \quad (4)$$

where $q_i = 10^{-0.05 L_{p,i}}$. Here, $L_{p,i}$ is the SPL measured in the i -th point and M is the total number of points along the measurement direction. Deviation of the measured SPL from theoretical predictions, defined as

$$\Delta L_p = L_{p,i} - L_p(r_i), \quad (5)$$

should not exceed the values listed in Tab. 2.

Figure 6(a) demonstrates spectral ranges (in the one-third octave band) and distances from the source for which the requirements for acoustic anechoic chambers are satisfied. To be specific, the cases where ΔL_p exceeds the feasible values are marked with red color on the diagram. Particular values are omitted for clarity, although it should be mentioned that the largest deviation reaches the value of 15.5 dB. In general, the chamber meets the requirements only for a limited set of frequencies and distances to the source. One of the reasons behind this result might be the non-uniform distribution of the absorbing coating throughout the chamber, as mentioned in its description. At the same time, the maps for deviations ΔL_p are not equivalent to each other, which might be an indication of the presence of scattering. Nevertheless, when the distance from the source is 0.5 – 0.8 m the chamber can be considered as an anechoic in the spectral range of 50 to 3150 Hz regardless of the measurement direction. The spectral range is much larger for directions III and IV, where the upper frequency limits are 16000 and 8000 Hz, respectively. Larger distances from the source to a measurement point imply larger deviations of the measured SPL from the corresponding theoretical values. It might be argued that the amplitudes of the

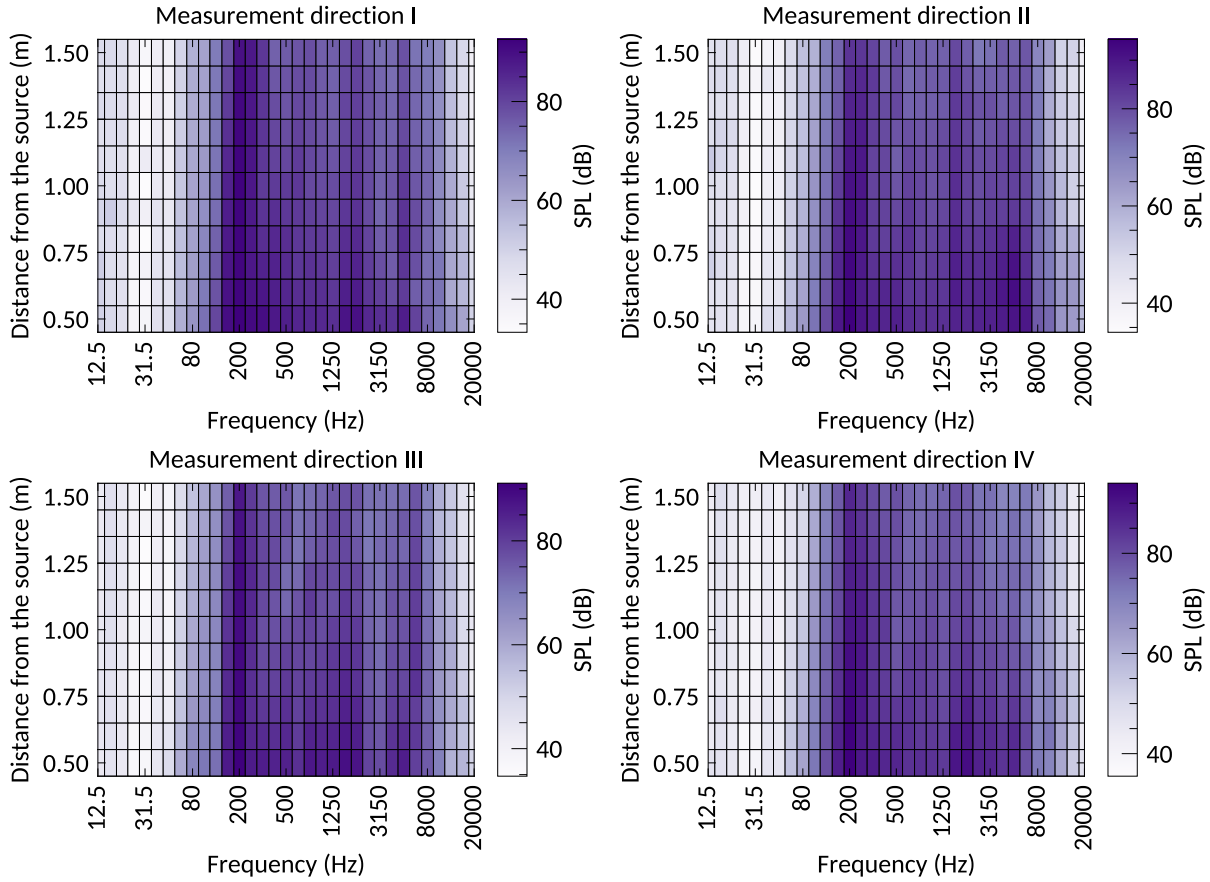


Figure 5: Measured sound pressure levels. Sound pressure level (SPL) spectra as functions of the distance from the source for different measurement directions.

reflected fields are much smaller than the amplitude of the generated field in the vicinity of the source. Hence, the distortions caused by the reflections are insignificant for the measurements near the source. For other distances, the contribution of the reflected fields becomes tangible, and consequently, the free-field conditions are satisfied only at some spectral ranges, which are listed in Tab. 3. It should be noted that when the overall SPL is considered, the deviation of the measured values from the theoretical ones does not exceed the level of ± 1 dB for all measurement directions except the direction II [see Fig. 6(b)]. Furthermore, the values of ΔL_p are below 0.6 dB for all distances from the source up to 0.8 m, which additionally indicates that the requirements for the anechoic chambers are satisfied.

5. Conclusion

The radiowave anechoic chamber of ITMO University (Saint-Petersburg, Russia) is analyzed for suitability criteria imposed on acoustic anechoic chambers. The results of the characterization indicate that the camera can be utilized for free-field acoustic measurements, in agreement with the ISO 3745:2012 / GOST-ISO 3745-2014 standard. However, it should be highlighted that the requirements defined by the standard are satisfied

Table 3

Frequency ranges and distances to the source for which the chamber can be considered anechoic.

Measurement direction	Frequency range (Hz)	Distance from the source (m)
I	50 – 3150	0.5 – 0.9
	50 – 125	1.0 – 1.4
	800 – 2000	1.0 – 1.4
II	50 – 1250	0.5 – 0.9
	1600 – 10000	0.5 – 0.8
	63 – 80	1.0 – 1.4
III	50 – 10000	0.5 – 0.9
	63 – 125	1.0 – 1.4
	1000 – 2000	1.0 – 1.3
IV	50 – 4000	0.5 – 0.9
	1600 – 2500	1.0 – 1.3

only for specific distances from the noise source and at limited frequency ranges, which are listed in Tab. 3.

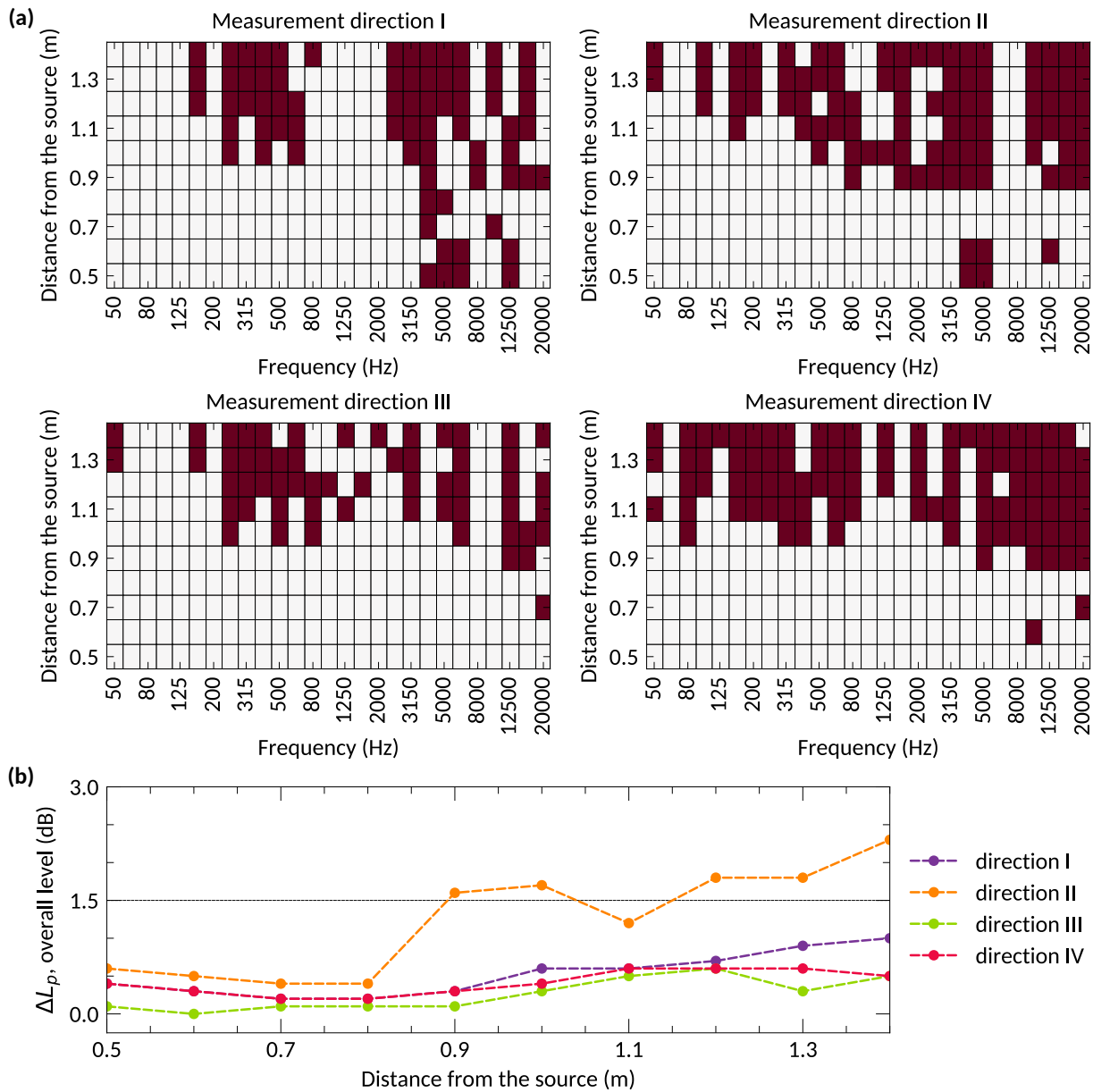


Figure 6: Camera compliance with suitability criteria. (a) Diagram indicating feasible deviation of the measured sound pressure level (SPL) from the corresponding theoretical predictions, ΔL_p , for different measurement directions. Color indicates the frequencies in one-third octave band and distances from the source at which the values of ΔL_p exceed the feasible limits defined for anechoic chambers (in accordance with Tab. 2). (b) Deviation of the measured overall SPL from the theoretical predictions.

Author Contributions

F.B. measured acoustic characteristics of absorbing coatings and processed the results. K.R., R.S., Y.S. and F.B. performed the measurements of sound pressure levels, background noise, and reverberation time of the chamber, K.R., R.S., and Y.S. processed the results. M.K. performed numerical calculations. M.K., Y.S. and N.K. supervised the work. All authors contributed to the analysis of the results and the preparation of the manuscript.

Declaration of Competing Interest

The authors declare that they have no known competing financial interests or personal relationships that could have appeared to influence the work reported in this paper.

Data availability

The data that support the findings of this study are available from the corresponding author upon reasonable request.

Acknowledgements

M.K. thanks Sergey Krasikov for useful discussions and comments.

References

- [1] Gerhard Müller and Michael Möser, editors. *Handbook of Engineering Acoustics*. Springer Berlin Heidelberg, Berlin, Heidelberg, 2013.
- [2] Leo L. Beranek and Tim J. Mellow. *Acoustics: Sound Fields, Transducers and Vibration*. Academic Press, London [England], second edition edition, 2019.
- [3] Edwin D. Burnett and Victor Nedzelnitsky. Free-Field Reciprocity Calibration Of Microphones. *Journal of Research of the National Bureau of Standards*, 92(2):129–151, 1987.
- [4] Allan J. Zuckerwar, G. C. Herring, and Brian R. Elbing. Calibration of the pressure sensitivity of microphones by a free-field method at frequencies up to 80kHz. *The Journal of the Acoustical Society of America*, 119(1):320–329, January 2006.
- [5] Thomas Rossing, editor. *Springer Handbook of Acoustics*. Springer Handbooks. Springer-Verlag, New York, 2 edition, 2014.
- [6] IEC 60118-0:2022. *Electroacoustics - Hearing aids - Part 0: Measurement of the performance characteristics of hearing aids*, 2022.
- [7] Janusz Piechowicz. Sound wave diffraction difference index for noise barrier with added device. *Vibrations in Physical Systems*, 34(2), 2023.
- [8] Vijaya Laxmi, Chaitanya Thakre, and Ritesh Vijay. Evaluation of noise barriers based on geometries and materials: a review. *Environmental Science and Pollution Research*, 29(2):1729–1745, 2022.
- [9] Ibrahim Ramadan, Tahra Salah, and Osama Alhariri. Studying the effect of noise barrier characteristics on traffic noise in urban areas. *Civil and Environmental Engineering*, 20(2):824–836, 2024.
- [10] Ablenya Barros, Jarl K Kampen, and Cedric Vuye. Noise barriers as a mitigation measure for highway traffic noise: Empirical evidence from three study cases. *Journal of environmental management*, 367:121963, 2024.
- [11] Qian Xu and Yi Huang. *Anechoic and Reverberation Chambers: Theory, Design, and Measurements*. Wiley-IEEE Press, 2019.
- [12] K.A. velizhanina and S.N. Rzhvekin. Research on sound-absorbing structures for the sound measurement chamber of the physics department of moscow state university. *Acoustic journal*, 3(1):23–28, 1957.
- [13] Kalustian R.T. Dombrovskiy R.V. Acoustic chamber with a wedge-shaped sound absorber made of fiberglass. 1962.
- [14] Dombrovskiy R.V. Industrial sound-absorbing coating for muffled sound measurement chambers. *Acoustic journal*, 12(4):484–485, 1966.
- [15] Ilkay Ozsev Yuksek and Nuray Ucar. Improvement of sound absorption coefficient of glass fiber fabric epoxy composite inherently without deterioration of main mechanical properties. *Polymers and Polymer Composites*, 30:09673911221086711, 2022.
- [16] Chunchun Zhang, Huiqin Li, Jixian Gong, Jiahao Chen, Zheng Li, Qiujin Li, Meilin Cheng, Xin Li, and Jianfei Zhang. The review of fiber-based sound-absorbing structures. *Textile Research Journal*, 93(1-2):434–449, 2023.
- [17] S. Yu. Makashov, S.U. Hramzov, I.V. Korin, I.A. Sorokin, and E.V. Kustov. Creation of a muffled installation for aeroacoustic experiments and study of its acoustic characteristics. *Acoustic journal*, 63(1):114–126, 2017.
- [18] Zhdanov M.A. Dombrovskiy R.V. Small acoustic anechoic chamber. *Acoustic journal*, 13(1):136–137, 1967.
- [19] B. M. Efimtsov and L. A. Lazarev. Sound Transmission Loss of Panels with Resonant Elements. *Acoustical Physics*, 47(3):291–296, May 2001.
- [20] Yu. I. Bobrovnikskii. Impedance theory of sound scattering and absorption: A constrained best absorber and the efficiency bounds of passive scatterers and absorbers. *Acoustical Physics*, 53(1):100–104, February 2007.
- [21] J Christian, Suprayogi, and N Fitriyanti. Absorber geometry size optimization for acoustic anechoic chamber design using genetic algorithm. In *Journal of Physics: Conference Series*, volume 2243, page 012085. IOP Publishing, 2022.
- [22] R Haasjes and AP Berkhoff. A solution method for active suppression of reflections in anechoic chambers. *The Journal of the Acoustical Society of America*, 157(1):569–578, 2025.
- [23] Elio Di Giulio, Raffaele Dragonetti, Rosario Aniello Romano, Annunziata Bruno, Jaime Guilherme Leal Guimarães Alves, and Antonio Scofano. Improvement of sound absorption of fibreglass structures. In *INTER-NOISE and NOISE-CON Congress and Conference Proceedings*, volume 272, pages 1995–2001. Institute of Noise Control Engineering, 2025.
- [24] Rivin A.N. Acoustic anechoic chamber. *Acoustic journal*, 7(3):324, 1961.
- [25] V. F. Kopiev, V. V. Palchikovskiy, I. V. Belyaev, Yu. V. Bersenev, S. Yu. Makashov, I. V. Khramtsov, I. A. Korin, E. V. Sorokin, and O. Yu. Kustov. Construction of an anechoic chamber for aeroacoustic experiments and examination of its acoustic parameters. *Acoustical Physics*, 63(1):113–124, January 2017.
- [26] Makov U.N. Vinogradov N.S. Changes in the acoustic characteristics of anechoic chambers with a removable sound-reflective work surface. *Acoustic journal*, 65(1):104–109, 2019.
- [27] Tuqa Khalid, Lutfi Albasha, Nasser Qaddoumi, and Sherif Yehia. Feasibility study of using electrically conductive concrete for electromagnetic shielding applications as a substitute for carbon-laced polyurethane absorbers in anechoic chambers. *IEEE Transactions on Antennas and Propagation*, 65(5):2428–2435, 2017.
- [28] Tom Ellam. An update on the design and synthesis of compact absorber for emc chamber applications. In *Proceedings of IEEE Symposium on Electromagnetic Compatibility*, pages 408–412. IEEE, 1994.
- [29] Yoshiyuki Naito, Tetsuya Mizumoto, Hiroki Anzai, and Michiharu Takahashi. Anechoic chamber fitted with ferrite grid or ferrite multi-layer electromagnetic wave absorbers. In *EMC'94 Roma, International Symposium on Electromagnetic Compatibility*, pages 229–234. IEEE, 1994.
- [30] Olga V Boiprav and Vadim A Bogush. Lightweight microwave absorbers with loop-like surface irregularities based on foiled materials for anechoic chambers. 2024.
- [31] Gita Rabelsa, Debi Rianto, Ananda Putra, Cahya Edi Santosa, Josaphat Tetuko Sri Sumantyo, et al. Pyramidal radar absorber based on coconut shell activated carbon for anechoic chamber application. In *2019 Photonics & Electromagnetics Research Symposium-Spring (PIERS-Spring)*, pages 1287–1291. IEEE, 2019.
- [32] Yue Shen and Gaoming Jiang. Sound absorption properties of composite structure with activated carbon fiber felts. *The Journal of The Textile Institute*, 105(10):1100–1107, 2014.
- [33] Amir Navidfar and Levent Trabzon. Fabrication and characterization of polyurethane hybrid nanocomposites: mechanical, thermal, acoustic, and dielectric properties. *Emergent Materials*, 5(4):1157–1165, 2022.
- [34] Santhanam Sakthivel, Selvaraj Senthil Kumar, Eshetu Solomon, Gedammesh Getahun, Yohaness Admassu, Meseret

- Bogale, Mekdes Gedilu, Alemu Aduna, and Fasika Abedom. Sound absorbing and insulating properties of natural fiber hybrid composites using sugarcane bagasse and bamboo charcoal. *Journal of Engineered Fibers and Fabrics*, 16:15589250211044818, 2021.
- [35] Olga Khrystoslavenko, Tomas Astrauskas, and Raimondas Grubliauskas. Sound absorption properties of charcoal made from wood waste. *Sustainability*, 15(10):8196, 2023.
- [36] Sichao Qu and Ping Sheng. Microwave and Acoustic Absorption Metamaterials. *Physical Review Applied*, 17(4):047001, April 2022.
- [37] Nansha Gao, Zhicheng Zhang, Xiao Liang, Yiting Li, and Guang Pan. Broadband multi-unit composite metamaterial for simultaneous sound wave and electromagnetic wave absorption. *Materials & Design*, 251:113671, March 2025.
- [38] ISO 3745:2012. Acoustics — Determination of sound power levels and sound energy levels of noise sources using sound pressure — Precision methods for anechoic rooms and hemi-anechoic rooms, 2012.
- [39] GOST ISO 3745:2014. Acoustics. determination of sound power levels and sound energy levels of noise sources using sound pressure. precision methods for anechoic rooms and hemi-anechoic rooms, 2015. Date of introduction: 2015-11-01.
- [40] ISO 10534-2:2023. Acoustics — determination of acoustic properties in impedance tubes — part 2: Two-microphone technique for normal sound absorption coefficient and normal surface impedance, 2023. Date of publication: 2023-10-06.
- [41] Michael E Delany and EN Bazley. Acoustical properties of fibrous absorbent materials. *Applied acoustics*, 3(2):105–116, 1970.
- [42] Jean-F Allard and Yvan Champoux. New empirical equations for sound propagation in rigid frame fibrous materials. *The journal of the acoustical society of America*, 91(6):3346–3353, 1992.
- [43] Massimo Garai and Francesco Pompili. A simple empirical model of polyester fibre materials for acoustical applications. *Applied Acoustics*, 66(12):1383–1398, 2005.
- [44] Yasushi Miki. Acoustical properties of porous materials-modifications of delany-bazley models. *Journal of the Acoustical Society of Japan (E)*, 11(1):19–24, 1990.
- [45] FP Mechel. Absorption cross section of absorber cylinders. *Journal of sound and vibration*, 107(1):131–148, 1986.
- [46] Trevor Cox and Peter D’Antonio. *Acoustic Absorbers and Diffusers: Theory, Design and Application*. CRC Press, Boca Raton, 3 edition, November 2016.
- [47] Sadao Aso and Rikuhiko Kinoshita. Sound absorption coefficient of glass wool. *Journal of the Textile Machinery Society of Japan*, 12(3):101–106, 1966.
- [48] Zhiting Feng and Yuanjun Liu. The latest research status of porous sound-absorbing materials. *Journal of Polymer Engineering*, 45(3):207–225, 2025.
- [49] Behzad Mohammadi, Amir Ershad-Langroudi, Gholamreza Moradi, Abdolrasoul Safaiyan, and Peymaneh Habibi. Mechanical and sound absorption properties of open-cell polyurethane foams modified with rock wool fiber. *Journal of Building Engineering*, 48:103872, 2022.
- [50] Xiao Liu, Chengyuan Wu, Haopeng Wang, Wangqiang Xiao, and Zhiqin Cai. Simulation and optimization of highly efficient sound-absorbing and-insulating materials. *Processes*, 13(9):2947, 2025.
- [51] Oshoke Wil Ikpekha and Mark Simms. Effect of acoustic absorber type and size on sound absorption of porous materials in a full-scale reverberation chamber. In *Acoustics*, volume 7, page 3. MDPI, 2025.